

Spectroscopy of Single Hemoglobin Molecules by Surface Enhanced Raman Scattering

Hongxing Xu, Erik J. Bjerneld, Mikael Käll,* and Lars Börjesson

Department of Applied Physics, Chalmers University of Technology, S-412 96 Göteborg, Sweden

(Received 22 January 1999)

We demonstrate the detection of molecular vibrations in single hemoglobin (Hb) protein molecules attached to isolated and immobilized silver nanoparticles by surface enhanced Raman scattering (SERS). A comparison between calculation and experiment indicates that electromagnetic field effects dominate the surface enhancement, and that single molecule Hb SERS is possible only for molecules situated between Ag particles. The vibrational spectra exhibit temporal fluctuations of unknown origin which appear to be characteristic of the single molecule detection limit.

PACS numbers: 82.65.Pa, 33.20.Fb, 42.62.Be, 87.64.-t

Single molecule spectroscopy (SMS) has the unique potential to probe how an individual molecule reacts to varying outer stimuli, and thus may provide detailed information inaccessible in ensemble averaged measurements. Until recently, optical SMS was essentially synonymous with single molecule fluorescence spectroscopy [1] and advances in this field over the past decade have indeed revealed a rich field of new physical phenomena [2]. However, compared to fluorescence, inelastic light scattering (Raman scattering), which can occur from vibrational excitations in all molecules, is a more general process which usually carries a higher information content. Although the ordinary Raman effect is extremely weak—typical cross sections are of the order 10^{-30} cm² per molecule—a dramatic signal enhancement may occur if the analyte molecule is adsorbed to metal particles of subwavelength dimensions. This technique, known as surface enhanced Raman scattering (SERS) [3], was recently employed by Nie and Emory [4] and Kneipp and co-workers [5,6], who demonstrated that the effective Raman cross section of small aromatic molecules could be increased by a staggering 14–15 orders of magnitude—a surface enhancement which proved enough for successful SMS.

In this Letter we present evidence of single molecule SERS for one important biological macromolecule: the oxygen transport protein hemoglobin (Hb). We find that the minimal aggregation number for effective SMS is the dimer, i.e., a pair of Ag nanoparticles bridged by a Hb molecule. We estimate the effective enhancement for such a “hot” site and compare the result with calculations of the local electric-field strength.

The SERS active silver colloid was prepared by citrate reduction of AgNO₃ according to Ref. [7], with NaCl (0.25 mM final concentration) added as an activation agent. The final Ag particle concentration in the solution was estimated to $\approx 3.5 \times 10^{-11}$ M. Adult human Hb obtained from Sigma Chemical Co. was incubated with the Ag hydrosol for ≈ 3 h in order to allow for efficient adsorption. In order to immobilize the SERS particles a droplet of the Hb/Ag solution was deposited on a polymer coated Si wafer [8] which was then rinsed in Milli-Q Plus

purified water. For a deposition time of a few seconds, a surface with well-separated Ag particles suitable for micro-Raman spectroscopy was obtained.

Figure 1 shows extinction spectra of the Ag colloid at various Hb concentrations. The broad and asymmetric double peak is typical of the combined absorption and Mie scattering spectrum from Ag particles of a size about $D \approx 100$ nm [9]. Whereas the pure hydrosol was found to be stable over a period of more than six months, the addition of even minute amounts of Hb resulted in aggregation. As can be seen from Fig. 1 the dominant effect is a reduction in optical density (OD) caused by a decrease in the number of scattering centers, but already at $[\text{Hb}] = 10^{-9}$ M an increase in OD at longer wavelengths signals large diameter colloidal aggregates. For even higher concentrations ($[\text{Hb}] > 10^{-7}$ M) the aggregation resulted in a precipitation of the colloid and the extinction spectrum became dominated by supernatant oxy/deoxy Hb absorption.

The Raman spectra were collected through a confocal optical microscope coupled to a single grating

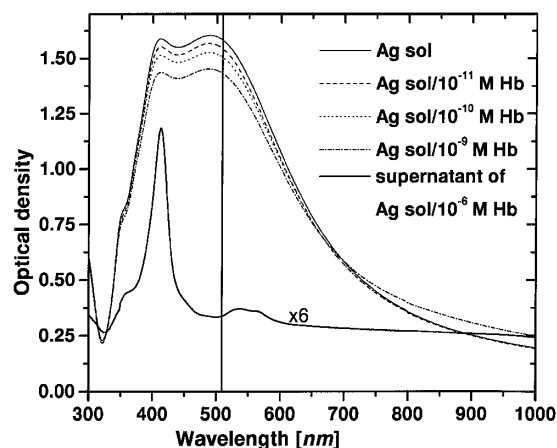


FIG. 1. Extinction spectra of Ag/Hb sols ($[\text{Hb}] = (0-10^{-9})$ M; 3 h incubation) together with supernatant Hb absorption after colloidal precipitation at $[\text{Hb}] = 10^{-6}$ M. The vertical line marks the incident laser wavelength ($\lambda_l = 514.5$ nm) used for Raman excitation.

spectrometer equipped with a notch filter and a CCD camera detector. Measurements were performed in backscattering geometry with the 514.5 nm Ar⁺ line as excitation, a laser spot size of $\sim 1 \mu\text{m}$ in diameter and a frequency resolution of $\approx 8 \text{ cm}^{-1}$ ($= 1 \text{ meV}$). An extremely low incident laser power (in the μW range) was used in order to minimize heating and photochemical effects.

The 5.5 nm diameter, nearly spherical Hb molecule contains four planar Fe-protoporphyrin prosthetic heme groups embedded in polypeptide chains in the form of two α -subunits and two β -subunits. The rich spectroscopic properties of Hb arise from π - π^* transitions within these heme groups, as is also the case for other heme proteins. Excitation at 514.5 nm results in a resonantly enhanced Raman spectrum dominated by in-plane porphyrin ring modes of the heme groups covering the frequency range 1100–1700 cm^{-1} [10].

In Fig. 2 we show a collection of Raman spectra from hemoglobin. Spectra *A* and *B* are “ordinary” Raman and SERS measurements, obtained from a Hb crystal facet and from a dense colloid film incubated with a surplus of hemoglobin, respectively. The positions and relative intensities of the Hb “marker” modes in *A* (at about 1375,

1586, and 1640 cm^{-1}) agree well with published data on met-Hb [10], whereas the positions in *B* indicate a transition to oxy/deoxy Hb [10], induced by the reduction agent present in the Ag hydrosol.

In order to reach the SMS limit it is necessary to use as low a concentration of analyte molecules as possible. Here we used $[\text{Hb}] = 1 \times 10^{-11} \text{ M}$, yielding a Hb-molecule-to-Ag-particle ratio of Hb:Ag $\approx 1:3$. This should ensure that only a very small number of Hb molecules adsorb to each investigated Ag particle. At this very low Hb concentration we find that only a few *hot sites* give rise to any detectable SERS intensity, in agreement with the study of Nie and Emory on rhodamine 6G [4].

Spectra *C* and *D* in Fig. 2 are examples of a time series of successive SERS spectra obtained from two such hot sites. The majority of the spectra (e.g., *C2*, *C4* and *D1*, *D3*) are in general agreement with the high-concentration SERS (*B*) and crystal Hb spectra (*A*), although there are clear differences in the precise peak positions and relative intensities. However, the most striking difference concerns the variation with time. Whereas spectra *A* and *B* are stable in time, the two time series obtained at extremely low analyte concentrations exhibit striking spectral fluctuations. In *C2*–*C4*, for example, a set of new intense peaks suddenly appears and disappears. A similar effect occurs in *D1*–*D3*, where a new peak at 1150 cm^{-1} seems to correlate with a broadening of the Hb marker modes. At present we are not able to present a detailed explanation of these temporal fluctuations. What is clear, however, is that their mere existence signals a *departure* from the normal time-invariant ensemble average. Together with the extremely small number of Hb molecules expected for each Ag particle complex, this strongly indicates that we have reached the single molecule detection limit.

Let us now consider the identification of the hot sites. After the Raman measurements of a particular sample were completed, the sample was brought to the scanning electron microscope (SEM) or atomic-force microscope (AFM) for inspection. Each individual Ag particle complex could easily be found and imaged by using markers on the Si wafer. The results of these investigations can be summarized as follows: (1) the Ag sol incubated with a $1 \times 10^{-11} \text{ M}$ Hb solution for 3 hours contained approximately 80% single particles, 15% dimers, and 5% triplets or larger aggregates, (2) of the more than 100 hot sites examined none consisted of a single Ag particle, and (3) the majority of the dimers/triplets found on SMS surfaces by SEM/AFM were hot in Raman. Moreover, among the hot dimers, those with their dimer axis oriented *parallel* to the incident electric field consistently produced the highest SERS intensity. In Fig. 3 we show some examples of Ag aggregates found in these investigations.

Although these findings might seem surprising at first glance, they are qualitatively anticipated from the

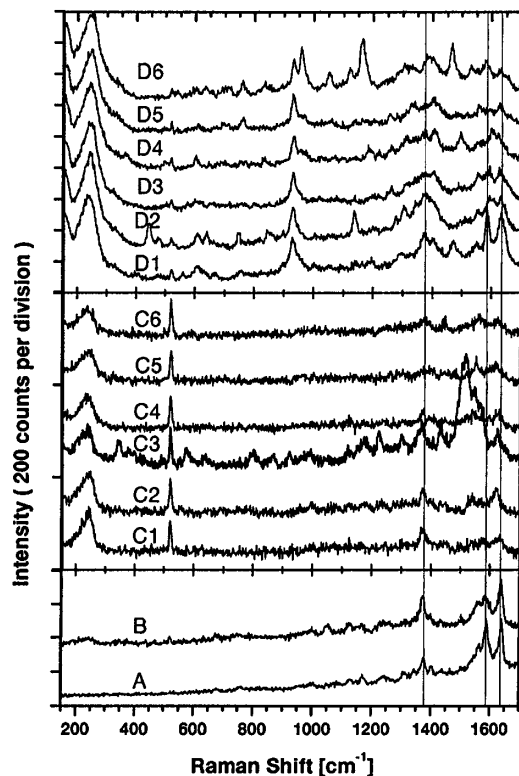


FIG. 2. Confocal Raman spectra of crystalline met-Hb (*A*), dense layer of Hb/Ag aggregates (*B*), and two time series (*C1*–*C6* and *D1*–*D6*) of “hot sites” obtained at the single molecule detection limit. The vertical lines indicate the Hb marker modes discussed in the text. All spectra were measured with the same collection time (30 s) and collection efficiency. The incident laser power was 1 mW in *A* and 1 μW in *B*–*D*.

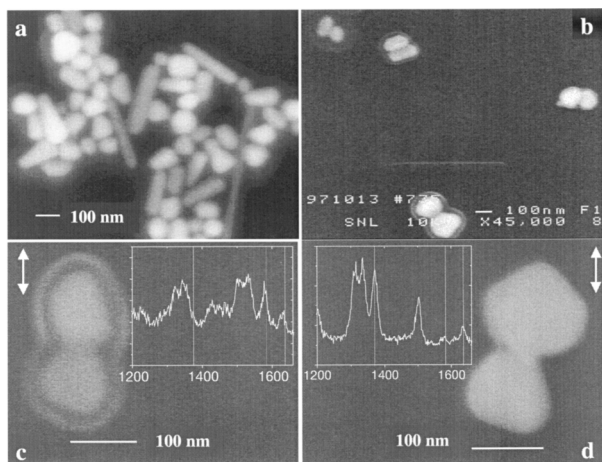


FIG. 3. SEM images of immobilized Ag particles. The pictures show (a) overview of Ag particle shapes and sizes, (b) Ag particle dimers observed after incubation with $1 \times 10^{-11} M$ Hb for 3 h, and (c),(d) hot dimers and corresponding single Hb molecule spectra. The double arrows in (c) and (d) indicate the polarization of the incident laser field.

“classical” electromagnetic theory of the SERS phenomenon [3]. We first recall, from the discussion of the extinction spectra given above, that Hb causes aggregation of the Ag sol. We thus have good reasons to suppose that the Ag particle aggregates, such as those depicted in Fig. 3, are actually *connected* by a Hb molecule.

In the classical description of SERS, the enhancement is caused by an amplification of the electric fields due to the coupling between the light and surface plasmons of the curved metal surface [3,11,12]. If one, for the sake of simplicity, assumes that the incident and scattered fields can be treated on an equal footing, one can express the enhancement factor $M = \sigma^{\text{SERS}}/\sigma^{\text{RS}}$, where σ^{SERS} and σ^{RS} are the molecular cross sections with and without the surface enhancement, as

$$M \approx |\vec{E}^L(\omega_I)/\vec{E}^I(\omega_I)|^2 |\vec{E}^L(\omega_I - \omega_v)/\vec{E}^I(\omega_I - \omega_v)|^2.$$

Here \vec{E}^I and \vec{E}^L are the incident electric field and the local electric field, respectively, in the presence of the metal. The frequency of the incident laser light and the vibrational frequency are denoted by ω_I and ω_v , respectively. The local field can be obtained from the integral equation

$$\vec{E}^L(\vec{r}, \omega) = \vec{E}^I(\vec{r}, \omega) + \int G(\vec{r}, \vec{r}') v(\omega, \vec{r}') \vec{E}^L(\vec{r}', \omega) d\vec{r}',$$

where $G(\vec{r}, \vec{r}')$ is the tensor Green function relating the electric fields at points \vec{r} and \vec{r}' . The potential $v(\omega, \vec{r}')$ is set to $(\omega/c)^2 \{\epsilon_0 - \epsilon_{\text{Ag}}(\omega)\}$ inside the Ag particle and zero outside. With the dielectric constant of silver taken from Ref. [13] and $\epsilon_0 = 1$ we have calculated M for the midpoint between two spheres of diameter D separated by a distance $d = 5.5$ nm, i.e., the diameter of a Hb

molecule. The calculations were performed according to the scheme developed by Inoue and Ohtaka [11], and we refer the interested reader to this article for mathematical details.

Figure 4 shows the results for $D = 60, 90,$ and 120 nm and \vec{E}^I either parallel or perpendicular to the dimer axis. For simplicity we have assumed a negligible Raman shift, i.e., $\omega_v = 0$. We also show the enhancement at a point situated $d/2$ nm outside an isolated sphere as a comparison. While the single particle enhancement is strongly peaked near the surface plasmon dipole resonance at about 400 nm, the dimer exhibits a second long-wavelength peak for the parallel configuration. As outlined by, e.g., Gersten and Nitzan [12], this second peak can be seen as the multipole broadened “bonding orbital” resulting from the mutual repulsion between the two single sphere dipole resonances. As can be seen from Fig. 4, the enhancement for the dimer system is approximately 4 orders of magnitude larger than for the single Ag sphere, if both are excited in the most favorable configuration. In contrast, excitation of the dimer in the perpendicular configuration results in an exclusion of the field between the spheres and consequently an enhancement factor below unity. In the inset of Fig. 4 we show the variation in enhancement with D for

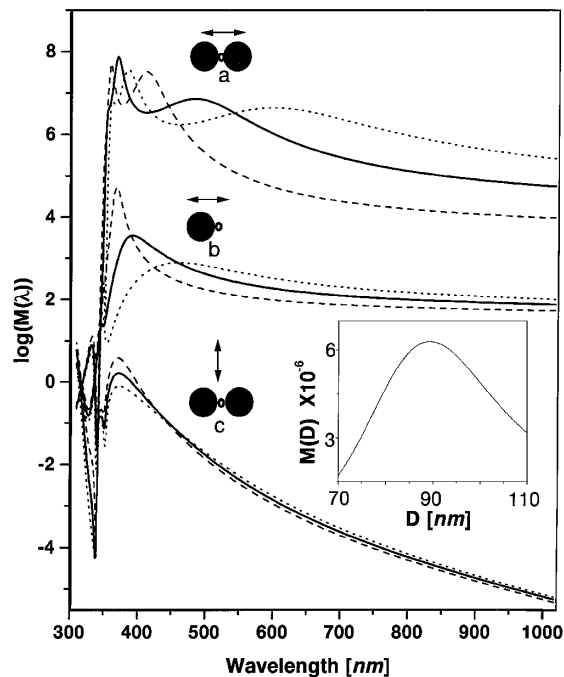


FIG. 4. Calculated electromagnetic enhancement factor for the midpoint between two Ag spheres separated by $d = 5.5$ nm and for a point $d/2$ outside a single sphere. The solid and open circles indicate the position of the Ag spheres and the Hb molecule, respectively, in relation to the incident polarization vector (double arrows). The calculations have been performed for spheres of diameters $D = 60$ (dashed curves), 90 (solid curves) and 120 nm (dotted curves). Inset shows the enhancement versus D for $\lambda_I = 514.5$ nm and a Stokes shift of 1500 cm^{-1} for configuration *a*.

the dimer in the parallel configuration. Here we have used $\omega_I = 514.5$ nm and $\omega_v = 1500$ cm⁻¹ in order to simulate the experimental situation. We find that the maximum enhancement occurs for spheres with a diameter of about 90 nm, in excellent agreement with the hot particle dimensions we observe experimentally. The question of interest is now whether the theoretically estimated maximum enhancement, $M \approx 6 \times 10^6$ from Fig. 4, is in agreement with an experimental estimate. From Fig. 2 we see that the intensity of the Hb marker modes are of similar magnitude in spectrum *A* and *D1*. As the collection efficiency is the same in both cases and the incident laser power is known, M is simply determined by the number of Hb molecules contributing to the total scattered intensity. For an illumination area of 1 μm^2 and a collection/illumination depth of 2 μm , these numbers are of the order $N^A \approx 1 \times 10^7$ and $N^{D1} \approx 1$, where we have assumed a close packed arrangement of Hb molecules in *A* and the SMS limit for spectrum *D1*. By taking into account the factor 10^3 difference in illumination intensity between *A* and *D1*, we obtain $M^{\text{SMS}} \approx 10^{10}$, i.e., more than 3 orders of magnitude higher than our calculated value for the ideal case. However, the field enhancement also depends critically on the distance d between the Ag particles. Changing d from 5.5 to 1 nm (with constants ω_I , ω_v , and D) results in an increase in M from $\approx 6 \times 10^6$ to $\approx 2.5 \times 10^{10}$. It is thus clear that the experimentally estimated enhancement factor is well within the reach of the electromagnetic model, even though we can not exclude that additional "chemical" charge transfer effects [14] contribute. One should also note that deviations from perfect sphericity may well increase the local field above that calculated above [3,12]. Calculations of these more complicated effects are underway and will be presented elsewhere.

Let us now briefly return to the temporal fluctuations described above. We note that spectral fluctuations of unknown origin were also observed in the single molecule SERS study of rhodamine 6G by Nie and Emory [4] and that similar effects are well known from SMS fluorescence studies (see, e.g., Ref. [2]). In the present case, it is unclear whether the effects are signs of spontaneous variations in the protein conformation and adsorption state, or whether photoinduced processes are involved. In the case of photochemical effects, which may be expected for illumination near the π - π^* Hb resonances, it is likely that both the electric-field enhancement and chemisorption processes could affect the photochemical yield [12]. It is also possible that photonic forces induced by the electric-field gradients near the Ag surfaces are contributing to

the fluctuations. It is clear that these effects could lead to conformational changes and, possibly, to the eventual disintegration of the protein, and therefore require considerable attention in future SMS studies by SERS.

In summary, we have obtained vibrational Raman spectra from single hemoglobin molecules attached to 100-nm-sized immobilized Ag particles. Our results indicate that Ag particle aggregation is a necessary condition for this effect, and that the observed protein molecules actually bind the Ag particle clusters together. We estimate the effective surface enhancement factor to $M^{\text{SMS}} \approx 10^{10}$, and argue that the dominant part of this enhancement is due to an increase of the local electric field between the Ag particles. The spectra exhibit temporal fluctuations which appear to be characteristic for the single molecule detection limit.

We thank Professor P. Apell, Dr. J. Aizpurua, and C. Tengroth for many stimulating discussions on the SERS effect. The financial support of the Swedish Foundation for Strategic Research is gratefully acknowledged.

*Corresponding author.

Email address: kall@fy.chalmers.se

- [1] W.E. Moerner and L. Kador, *Phys. Rev. Lett.* **62**, 2535 (1989).
- [2] For a review of the SMS field, see *Single-Molecule Optical Detection, Imaging and Spectroscopy*, edited by T. Basché *et al.* (VCH, Weinheim, 1996).
- [3] For a review, see M. Moskovits, *Rev. Mod. Phys.* **57**, 783 (1985).
- [4] S. Nie and S.R. Emory, *Science* **275**, 1102 (1997).
- [5] K. Kneipp *et al.*, *Phys. Rev. Lett.* **78**, 1667 (1997).
- [6] K. Kneipp *et al.*, *Phys. Rev. E* **57**, 6281 (1998).
- [7] P.C. Lee and D. Meisel, *J. Phys. Chem.* **86**, 3391 (1982).
- [8] We used a self-assembled monolayer of APTMS, as described by R.G. Freeman *et al.* [*Science* **267**, 1629 (1995)].
- [9] For a review, see U. Kreibig and M. Vollmer, *Optical Properties of Metal Clusters* (Springer, New York, 1995).
- [10] For a review, see T.G. Spiro, in *Iron Porphyrins, Part II*, edited by A.B.P. Lever and H.B. Gray (Addison-Wesley, London, 1983).
- [11] M. Inoue and K. Ohtaka, *J. Phys. Soc. Jpn.* **52**, 3853 (1983).
- [12] J.I. Gersten and A. Nitzan, *Surf. Sci.* **158**, 165 (1985).
- [13] P.B. Johnson and R.W. Christy, *Phys. Rev. B* **6**, 4370 (1972).
- [14] B.N.J. Persson, *Chem. Phys. Lett.* **82**, 561 (1981).